

Particle entrapment as a feedback effect

Sergey V. Shklyaeu

Theoretical Physics Department, Perm State University, Bukirev 15, 614990 Perm, Russia

Arthur V. Straube

Department of Physics, University of Potsdam, Am Neuen Palais 10, PF 601553, D-14415 Potsdam, Germany

(Dated: August 25, 2021)

We consider a suspension of polarizable particles under the action of traveling wave dielectrophoresis (DEP) and focus on particle induced effects. In a situation where the particles are driven by the DEP force, but no external forces are exerted on the fluid, the joint motion of the particles can induce a steady fluid flow, which leads to particle entrapment. This feedback effect is proven to be non-negligible even for small volume concentration of particles.

PACS numbers: 47.55.Kf, 47.61.-k, 47.15.Fe, 47.54.+r

Recent progress and numerous applications in medicine, biotechnology and pharmaceutical research have witnessed a great interest in understanding of fundamental aspects of particle dynamics in fluid flows at small scales [1]. Particularly, the concept of particle manipulation is an important problem of micro- and nanofluidics [2]. Here, the particles can be physical (colloids, liquid droplets in microemulsions, small bubbles) or biological (cells, bacteria, biopolymers) objects manipulated with e.g., electrokinetic [3], magnetic forces [4], ultrasound [5] or optical tweezers [6]. Despite a considerable success in understanding of the impact of hydrodynamic [3, 7] and stochastic [8] forces on the particle dynamics, the problem of backward coupling, i.e., the influence of the particle dynamics on the fluid, or *particle feedback*, includes a number of open questions. Especially challenging is the problem of *integral* feedback effects that can be induced by a collection of *jointly* moving particles. In this Letter, we systematically address this problem. We introduce an original theoretical model, apply it to a physically realistic problem, and predict a generic mechanism of particle entrapment that is fundamentally different to the ones conventionally known [9, 10, 11].

We start with the formulation of a continuum model for spherical noninteracting particles of radius a suspended in a fluid having viscosity η and density ρ . To focus on the feedback effects we impose a nonuniform external force $F_0 \mathbf{F}(\mathbf{r})$ on the particles (F_0 its reference value and \mathbf{F} is the dimensionless field), which, however, does not directly influence the carrier phase. Provided that the relative size of particles a/L (L is the length scale of the flow) and their space-averaged volume fraction Φ_0 are small, the dynamics of the two-phase system is described by a model allowing for the feedback [12]:

$$\frac{1}{Sc} \left(\frac{\partial \mathbf{u}}{\partial t} + \mathbf{u} \cdot \nabla \mathbf{u} \right) = -\nabla p + \nabla^2 \mathbf{u} + Q_s \langle \Phi \rangle \varphi \mathbf{F}, \quad (1)$$

$$\text{div } \mathbf{u} = 0, \quad \mathbf{v} = \mathbf{u} + Q_s \mathbf{F}, \quad (2)$$

$$\frac{\partial \varphi}{\partial t} + \text{div } \mathbf{j} = 0, \quad \mathbf{j} = \varphi \mathbf{v} - \nabla \varphi, \quad (3)$$

where \mathbf{u} and \mathbf{v} are the fluid and particle velocities, respectively, p is the pressure, φ is the particle volume fraction, and \mathbf{j} is the particle flux. The equations have been nondimensionalized using the scales L , L^2/D , D/L , $\eta D/L^2$, Φ_0 (D is the particle diffusivity) for the length, time, velocity, pressure, and particle volume fraction, respectively. Here $Q_s = 2a^2 L F_0 / 9\eta D$ stands for the intensity of the external field, $Sc = \eta / D\rho$ is the Schmidt number, and a ratio of two asymptotically small parameters $\langle \Phi \rangle = 9L^2 \Phi_0 / 2a^2$ is the feedback parameter, which is assumed to be finite.

To stress the relevance of our approach hereafter we provide estimations for a realistic system. As example, we stick to the data close to experimental [3]. For a water ($\eta \simeq 10^{-2}$ g/cm s, $\rho \simeq 1$ g/cm³) suspension with $a \simeq 200$ nm and $\Phi_0 \simeq 3\%$ in a container of the size $2L \simeq 25$ μ m at temperature 300 K one obtains $\langle \Phi \rangle \simeq 500$ and according to Einstein's formula $D \simeq 10^{-8}$ cm²/s and $Sc \simeq 10^6$. Although in most conventional situations Sc is high, it becomes necessary to account for the diffusion of particles. The reason is twofold: (i) even small diffusion gets non-negligible at small scales, e.g., the diffusion time is of order $L^2/D \simeq 100$ s; (ii) it prevents from unbounded physically irrelevant accumulation of particles by the external field.

We emphasize that only particles are able to make fluid move, i.e., the fluid flow itself is a perfect indicator for the particle feedback, described by the last term in Eq. (1). Physically, this term comes from the Stokes drag, which dominates in the interphase force [10, 13] and is balanced by \mathbf{F} . Particularly, this results in a distinction of the velocities of phases, where inertia corrections are negligible.

Further we focus on an example of a dielectrophoretic (DEP) force exerted on polarizable particles under ac electric field $\mathbf{E}(\mathbf{r}, t) = \text{Re}[\tilde{\mathbf{E}}(\mathbf{r}) \exp(i\omega t)]$. Hereafter ω is the angular frequency, $i = \sqrt{-1}$, $\text{Re}[z] \equiv z_r$ and $\text{Im}[z] \equiv z_i$ denote the real and imaginary parts of z . The time-averaged force (per unit volume) reads [3]:

$$F_0 \mathbf{F} = \frac{3}{2} \epsilon_m \text{Re} \left[\tilde{K}(\omega) \tilde{\mathbf{E}} \cdot \nabla \tilde{\mathbf{E}}^* \right], \quad (4)$$

where “*” indicates complex conjugate. The complex frequency-dependent function $\tilde{K}(\omega) = (\tilde{\epsilon}_p - \tilde{\epsilon}_m)/(\tilde{\epsilon}_p + 2\tilde{\epsilon}_m)$ is a measure of an effective polarizability of the particle, known as the Clausius-Mossotti factor. Here, $\tilde{\epsilon}_p$ and $\tilde{\epsilon}_m$ are the complex permittivities of the particles and the fluid medium, respectively. The complex permittivity is defined as $\tilde{\epsilon} = \epsilon - i\sigma/\omega$ (ϵ is the permittivity and σ is the conductivity of the dielectric). The DEP force (4) comprises two independent contributions:

$$F_0 \mathbf{F} = \frac{3}{4} \epsilon_m \tilde{K}_r \nabla |\tilde{\mathbf{E}}|^2 - \frac{3}{2} \epsilon_m \tilde{K}_i \nabla \times (\tilde{\mathbf{E}}_r \times \tilde{\mathbf{E}}_i). \quad (5)$$

The first term relates to the in-phase component of the induced dipole. This force points towards the domains of higher field strength for $\tilde{K}_r > 0$ or, conversely, to the domains of weaker fields for $\tilde{K}_r < 0$, which is referred to as *positive-DEP* (*p-DEP*) or *negative-DEP* (*n-DEP*), respectively [14]. The particles are attracted or repelled by the electrode edges. The second term is due to the out-of-phase component of the dipole and is essential if there is spatially varying phase [3], e.g., for traveling wave DEP; it makes the particles move parallel to the electrodes.

To be able to focus on the feedback effects one has to carefully ensure that these are not hindered by other possible sources of fluid motion. Because of Joule heating, applied electric fields induce temperature gradients and therefore create nonuniformities of the conductivity, permittivity and density in the fluid, which can lead to electroconvection and/or natural convection [3]. A typical electrothermal force on the fluid $F_{ET} \propto \sigma_m U_0^4 L^{-3}$ is negligible compared to the feedback term, provided that $F_{ET}/F \propto \sigma_m U_0^2 / \Phi_0 \ll 1$ (U_0 is a characteristic value of the electric potential). This requirement can be safely satisfied for weak fields or weakly conductive fluids. Further we assume that the last option is met, e.g., for pure water ($\sigma_m \simeq 30 \mu\text{S}/\text{cm}$), or deionized water ($\sigma_m \simeq 2 \mu\text{S}/\text{cm}$) applied in [11], and $U_0 \simeq 0.1 \text{ V}$ we obtain F_{ET}/F of order 10^{-5} or 10^{-6} , respectively. As we claim below, considerably weaker fields are enough to cause the feedback-induced flow (cf. with $U_0 \simeq 1 - 10 \text{ V}$ in [3, 11, 15]). One more advantage of the low conductivity is that ac electro-osmosis (another electrohydrodynamic effect that can induce a flow caused by electrical stresses in the diffuse double layer of charges near the electrodes) and natural convection are even weaker than electroconvection.

We now turn to the analysis of a system typical for experiments on traveling wave DEP [3, 15]. Consider the two-phase medium filling a rectangular container of sizes L_x , $L_y \equiv 2L$, L_z and impose a traveling wave of the potential at the boundaries $y = \pm L$: $\phi = U_0 \exp[i(\omega t - qx)]$, where q is the wave number and U_0 is the amplitude. The complex amplitude $\tilde{\phi}(\mathbf{r})$ ($\tilde{\mathbf{E}} = -\nabla \tilde{\phi}$) obeys the Laplace equation, $\nabla^2 \tilde{\phi} = 0$, which is readily solved. Assuming that $L_y \ll L_x$, $L_y \ll L_z$ and that the sidewalls are electrically passive, we obtain

$\tilde{\phi}(\mathbf{r}) = U_0 \exp(-iqx)(\cosh qy)/\cosh qL$ and evaluate

$$\mathbf{F}(\mathbf{r}) = (-K_i \cosh by, \sinh by, 0). \quad (6)$$

Here we define $F_0 = 3\epsilon_m U_0^2 q^3 \tilde{K}_r / 2 \cosh^2(b/2)$ and introduce a dimensionless parameter $K_i = \tilde{K}_i / \tilde{K}_r$ and the dimensionless wavenumber $b = 2qL$. A traveling wave of a period $50 \mu\text{m}$ leads to $b \approx 3$ and $|Q_s| \approx 0.5$ (estimations are based on the data as before). Next, we restrict our consideration to the case of $K_i > 0$ as reversal of the sign of K_i changes the direction of the induced flow.

We first point out to a partial case of $K_i = 0$, which corresponds to the limit of perfectly lossless dielectric particles. According to (6), there is no force allowing for the particle transport along the plates $y = \pm 1$, only transversal redistribution occurs. The particles tend to migrate either towards or away from these boundaries, which is counterbalanced by diffusion; longitudinal nonuniformities are smeared by diffusion. Thus, this situation admits a state of *mechanical equilibrium* described by the quiescent fluid $\mathbf{u}_0(\mathbf{r}) = 0$, vanishing particle flux $\mathbf{j}_0(\mathbf{r}) = 0$, and a nonuniform distribution of particles

$$\varphi_0(\mathbf{r}) = C_0 \Psi_0(y), \quad \Psi_0(y) = \exp(Q_s b^{-1} \cosh by), \quad (7)$$

where $C_0 = 1 / \int_0^1 \Psi_0(y) dy$, as by definition the averaged φ is unity. The concentration profile (7) describes accumulation of particles near the boundaries for $Q_s > 0$, or in the center plane for $Q_s < 0$, which corresponds to *p-DEP* or *n-DEP*, respectively. Analytical and numerical treatment of the linearized problem as well as a direct numerical simulation (DNS) of the nonlinear model (1)-(3) with (6) indicate that the state of mechanical equilibrium is stable for any values of the governing parameters.

What happens in a more general case of lossy particles, when $K_i \neq 0$ and the longitudinal transport is allowed, is a simple question to pose, but the remarkably hard one to answer. In the limiting case of no feedback, $\langle \Phi \rangle \ll 1$, there is no source for fluid motion and the problem reduces to finding a distribution $\varphi_0(\mathbf{r}) = \varphi_0(x, y)$, governed by Eqs. (2), (3) with $\mathbf{u}(\mathbf{r}) = 0$. In the presence of the feedback, the problem becomes highly nontrivial, because the system is mechanically nonequilibrium. To get an impression of possible scenarios, we have numerically integrated Eqs. (1)-(3) with (6) in a two-dimensional rectangular box with the no-slip condition for \mathbf{u} and vanishing normal component for \mathbf{j} at the solid walls. A typical steady state solution is presented in Fig. 1. The flow is of a large scale and closed, the particles are involved in the vortical motion, which is reminiscent of the particle entrapment under gravity by Stommel [9] (for high aspect ratio see Ref. 16). However, there are two principal differences. First and most important, the conventional entrapment implies existence of a vortex flow irrespective of whether there are any particles or not [9, 10, 11, 16]. The fluid flow in our system can be induced only by means of particles and is not possible otherwise. In contrast to the

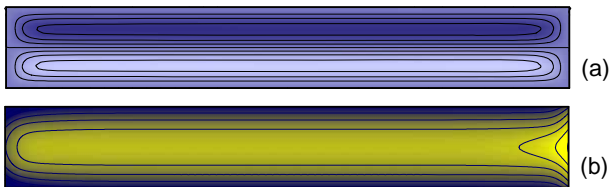


FIG. 1: (Color online). Contourplots of the streamfunction (a) and particle concentration (b) in the steady state for $Sc = 2$, $Q_s = -0.2$, $K_i = 1$, $b = 3$, $\langle \Phi \rangle = 575$. Lighter (clockwise rotation for vortices) and darker (counterclockwise rotation) colored domains refer to higher and lower values of the plotted fields, respectively. Steady states corresponding to different Sc look similar: a slight distinction comes from the nonlinear term, which is nonvanishing only near the sidewalls.

previous studies, particle entrapment arises as a generic particle feedback effect, which also provides a way to generate a flow. The second important distinction is that we carefully account for the diffusion effects. This nontrivial problem has been systematically addressed neither in studies cast into a Hamiltonian frame [9, 10, 16], nor in a non-Hamiltonian system [11].

A closer inspection of Fig. 1 shows that the flow and concentration patterns are one dimensional (1D) everywhere except for the vicinities of the sidewalls. This allows for a 1D analysis of Eqs. (1)-(3) with (6) away from the sidewalls, valid for systems with a high aspect ratio. Accordingly, we apply the ansatz $\varphi_0(\mathbf{r}) = \varphi_0(y)$, $\mathbf{u}_0(\mathbf{r}) = (u_0(y), 0, 0)$. As the flow does not influence the distribution of particles, $\varphi_0(y)$ is given by (7) with the same C_0 . To determine the fluid velocity we account for the no-slip conditions at the solid walls $u_0(\pm 1) = 0$ and a condition of no mean fluid flux $\int_{-1}^1 u_0 dy = 0$, implying that the flow is closed. As a result, we obtain:

$$u_0(y) = \alpha V_0(y), \quad V_0(y) = V_{01}(y) + V_{02}(y) \quad (8)$$

with $V_{01}(y) = I_2(1) - I_2(y)$, $V_{02}(y) = -\beta(1 - y^2)$, where $\alpha = C_0 \langle \Phi \rangle |Q_s K_i| > 0$, $\beta = 3[I_2(1) - I_3(1)]/2 > 0$, $I_1(y) = \int_0^y \Psi_0(\xi) \cosh b\xi d\xi$, and $I_{l+1}(y) = \int_0^y I_l(\xi) d\xi$ ($l = 1, 2$); because of symmetry, $V_0(y)$ is an even function. Next, we impose the condition of particle entrapment $\int_{-1}^1 \mathbf{j}_0 \cdot \mathbf{e}_x dy = 0$, $\mathbf{e}_x = (1, 0, 0)$, which ensures no mean particle flux [16]. We arrive at

$$\langle \Phi \rangle = I_1(1) \left(C_0 \int_0^1 V_0 \Psi_0 dy \right)^{-1} \equiv \langle \Phi \rangle_c, \quad (9)$$

representing a formal restriction on $\langle \Phi \rangle$: for every set of governing parameters, only a specific number of particles defined by (9) can be maintained trapped by the flow. In practice, however, e.g., for a closed rectangular box, such a restriction is not stringent. For $\langle \Phi \rangle$ different from $\langle \Phi \rangle_c$, the solution away from the sidewalls still corresponds to (7), as if $\langle \Phi \rangle = \langle \Phi \rangle_c$. Their actual distinction is balanced in the vicinities of the sidewalls, where the lack or excess

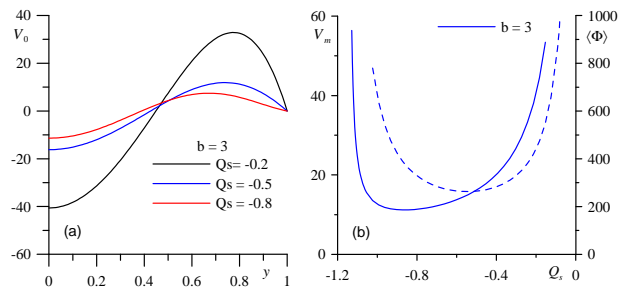


FIG. 2: (Color online). Characteristics of 1D state of entrapment (7)-(9) for $b = 3$: velocity profiles (a), maximal absolute velocity $V_m = \max_y |V_0(y)|$ and $\langle \Phi \rangle_c$ as functions of Q_s (b).

of particles emerges leading to local gradients of concentration on top of (7). This is clearly seen in Fig. 1(b). Of special attention is the case of $\langle \Phi \rangle$ considerably smaller than $\langle \Phi \rangle_c$. Here, although there are not enough particles to excite the flow in the whole domain, the entrapment still occurs. As before, it is accompanied by the birth of a steady vortex flow, but of a smaller longitudinal extension. With the decrease of $\langle \Phi \rangle$ the vortices gradually shrink and in the limit of $\langle \Phi \rangle \ll 1$ no longer exist.

The characteristics of the discussed state are presented in Fig. 2. The particles tend to move along the axis x , faster near the boundaries and slower at the center of the channel [see Eqs. (2) and (6)]. Because of viscous drag, the fluid is towed by the particles, which has two consequences. First, this motion contributes in a positive fluid flux, defined by $V_{01}(y)$. Second, it creates a longitudinal gradient of pressure that gives rise to an opposite Poiseuille flow $V_{02}(y)$ with the maximal velocity at the center. The velocity profile $V_0(y)$ is a superposition of these counterflows, such that the net fluid flux is vanishing. Noteworthy, profile (8) qualitatively resembles the one in the convective flow in a vertical slot induced by internal sources of heat [17]. In our case, the role of the heat sources is played by the nonuniform distribution of particles and the DEP force instead of gravity. Note, the state of entrapment exists only for $Q_c < Q_s < 0$, see Fig. 2(b). Beyond this range, Eq. (9) prescribes negative values of $\langle \Phi \rangle_c$, which is physically irrelevant. Particularly, this manifests that the entrapment can be observed only for n -DEP. From the experimental point of view, the flow can be easily controlled by tuning the frequency of the imposed traveling wave.

Next question concerns existence of the revealed effect in real systems. To answer it, we have linearized Eqs. (1)-(3) near solution (7), (8) and investigated its stability with respect to perturbations of the form $f(\mathbf{r}) = \hat{f}(y) \exp(\lambda t - ik_x x - ik_z z)$. Here $\lambda = \lambda_r + i\lambda_i$ is the complex growth rate, k_x and k_z are the wave numbers along axes x and z , respectively. The analysis has shown that the modes with the largest λ_r correspond to the perturbations in the form of rolls, $k_z = 0$. We have

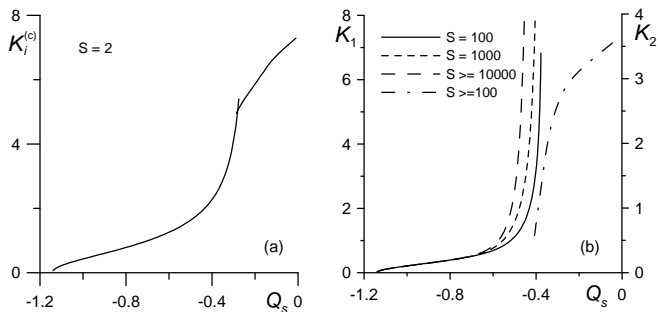


FIG. 3: Stability map for $b = 3$, $Sc = 2$ (a). Scaling functions $K_1(Q_s)$ and $K_2(Q_s)$ for different Sc (b).

checked a wide range of Schmidt numbers $1 < Sc < 10^6$ and found no qualitative changes, the stability maps are presented in Fig. 3. The regions of stable and unstable behavior are separated by two curves $K_i^{(c)}(Q_s)$ of neutral stability, on which $\lambda_r = 0$. These lines refer to a pair of competing modes of the largest λ_r , and have different asymptotes for $Sc \gg 1$. For the branches with higher and lower $|Q_s|$ the scaling laws are $K_i^{(c)} = K_1 \sqrt{Sc}$ and $K_i^{(c)} = K_2 Sc$, respectively. The dependencies $K_1(Q_s)$ and $K_2(Q_s)$ for different Sc are plotted in Fig. 3(b). With the growth of Sc , these dependencies converge to master curves. Because of the different scaling, the convergence of K_1 is slower, whereas K_2 gets indistinguishably close to its master curve already at $Sc = 100$.

The results of the linear stability analysis were confirmed by DNS of the nonlinear model (1)-(3) with (6). Note, as for large Sc the value $K_i^{(c)}$ is high, the instability in this particular situation is hardly reachable experimentally. However, it can be the case for moderate Sc . We have studied the breakdown of the 1D state, which is found to occur supercritically. The patterns beyond the threshold (see Fig. 4 for a snapshot) travel along the axis x with a speed λ_i/k_x . For the different branches the patterns look similar, but have distinct spatial periods and travel in opposite directions.

In conclusion, we have studied the role of the particle feedback in a two-phase system under the action of traveling wave DEP. In a situation where the particles are driven by the DEP force but no external forces are exerted on the fluid, the joint motion of the particles can induce a steady fluid flow, which is accompanied by novel particle entrapment. In a contrast to the conventional mechanism, diffusion of the particles becomes a necessary ingredient for the entrapment. This particle feedback effect has been proven to be non-negligible even for small volume concentration of particles. We note that similar phenomena are expected to exist in various physical systems. Indeed, the set of Eqs. (1)-(3) with the force in the form (4) describe a wide class of problems, e.g., magne-

tized ferrofluids [18], particles driven by optical tweezers [6], bubbly fluids under vibrations [19], where the field \vec{E} entering (4) is of different nature.

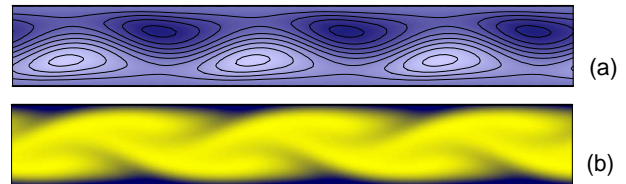


FIG. 4: (Color online). Breakdown of 1D state beyond the stability threshold, $Sc = 2$, $Q_s = -0.2$, $K_i = 7$, $b = 3$, $\langle \Phi \rangle = 450$: streamfunction (a) and particle concentration (b).

We acknowledge fruitful discussions with A.A. Nepomnyashchy, A. Pikovsky, B. L. Smorodin, V. Steinberg, and C. Pooley. S.S. thanks DAAD for support; A.S. was supported by the German Science Foundation (DFG, SPP 1164 “Nano- and microfluidics,” project 1021/1-1).

-
- [1] G. M. Whitesides, *Nature (London)* **442**, 368 (2006).
 - [2] T. M. Squires and S. R. Quake, *Rev. Mod. Phys.* **77**, 977 (2005).
 - [3] H. Morgan and N. G. Green, *AC Electrokinetics: Colloids and Nanoparticles* (Research Studies Press, Baldock, 2003); A. Ramos, H. Morgan, N. G. Green, and A. Castellanos, *J. Phys. D* **31**, 2338 (1998).
 - [4] M. A. M. Gijs, *Microfluidics & Nanofluidics* **1**, 22 (2004).
 - [5] J. J. Hawkes et al. *J. Phys. D* **31**, 1673 (1998).
 - [6] D. G. Grier, *Nature (London)* **424**, 810 (2003).
 - [7] S. Kim and S. J. Karrila, *Microhydrodynamics: Principles and Selected Applications* (Butterworth-Heinemann, Boston, 1991).
 - [8] P. Reimann and P. Hänggi, *Appl. Phys. A* **75**, 169 (2002); P. Reimann, *Phys. Rep.* **361**, 57 (2002).
 - [9] H. Stommel, *J. Mar. Res.* **8**, 24 (1949).
 - [10] M. R. Maxey, *Phil. Trans. R. Soc. London A* **333**, 289 (1991).
 - [11] I. Tuval et al. *Phys. Rev. Lett.* **95**, 236002 (2005).
 - [12] Details will be published elsewhere; for approach see Refs. 13, 16, 19
 - [13] O. A. Druzhinin, *J. Fluid Mech.* **297**, 49 (1995).
 - [14] H. A. Pohl, *Dielectrophoresis* (Cambridge University Press, Cambridge, England, 1978).
 - [15] M. Felten, P. Geggier, M. Jäger, and C. Duschl, *Phys. Fluids* **18**, 051707 (2006).
 - [16] D. V. Lyubimov, A. V. Straube, and T. P. Lyubimova, *Phys. Fluids* **17**, 063302 (2005).
 - [17] G. Z. Gershuni and E. M. Zhukhovitsky, *Convective Stability of Incompressible Fluid* (Keter, Jerusalem, 1976).
 - [18] M. I. Shliomis and B. L. Smorodin, *J. Magn. Magn. Mater.* **252**, 197 (2002).
 - [19] A. V. Straube, D. V. Lyubimov, and S. V. Shklyaev, *Phys. Fluids* **18**, 053303 (2006).